Quasi 18-hour wave activity in ground-based observed mesospheric H_2O over Bern, Switzerland

Martin Lainer[1], Klemens Hocke[1,2], Rolf Rüfenacht[1,3], and Niklaus Kämpfer[1,2]

[1]Institute of Applied Physics, University of Bern, Bern, Switzerland
[2]Oeschger Center for Climate Change Research, University of Bern, Bern, Switzerland
[3]Actual affiliation: Leibniz-Institute of Atmospheric Physics, Kühlungsborn, Germany

Correspondence to: M. Lainer (martin.lainer@iap.unibe.ch)

Abstract. Observations of oscillations in the abundance of middle atmospheric trace gases can provide insight into the dynamics of the middle atmosphere. Long term, high temporal resolution and continuous measurements of dynamical tracers within the strato- and mesosphere are rare, but would be important to better understand the impact of atmospheric waves on the middle atmosphere. Here we report on water vapor measurements from the ground-based microwave radiometer MIAWARA located close to Bern during two winter periods of 6 months from October to March. Oscillations with periods between 6 and 30 hours are analyzed in the pressure range 0.02–$2\,\mathrm{hPa}$. Seven out of twelve months have the highest wave amplitudes between 15 and 21 hour periods in the mesosphere above $0.1\,\mathrm{hPa}$. The quasi 18-hour wave signature in the water vapor tracer is studied in more detail by analyzing its temporal evolution in the mesosphere up to an altitude of $75\,\mathrm{km}$. 18-hour oscillations in mid-latitude zonal wind observations from the microwave Doppler wind radiometer WIRA could be identified within the pressure range 0.1–$1\,\mathrm{hPa}$ during an ARISE (Atmospheric dynamics Research InfraStructure in Europe) affiliated measurement campaign at the Observatoire de Haute-Provence ($355\,\mathrm{km}$ from Bern) in France in 2013. The origin of the observed upper mesospheric quasi 18-hour oscillations is uncertain and could not be determined with our available data sets. Possible drivers could be low frequency inertia-gravity waves or a non-linear wave-wave interaction between the quasi 2-day wave and the diurnal tide.

1 Introduction

The dynamics of the middle atmosphere is controlled by a broad spectrum of waves. Knowledge about the wave characteristics and incidence is important, not only to better understand the elements of middle atmospheric dynamics, but carrying on to improve predictions of weather (Hardiman et al., 2011) and climate (Orr et al., 2010) models. Latter are getting more important since the social impact of severe weather events and climate change is increasing.

Waves with horizontal wavelengths reaching thousands of kilometers and showing periods up to several weeks are classified as planetary waves. A well-known class of planetary waves are Rossby waves (Salby, 1981b). Their periods range from 2 to approximately 18 days in the middle atmosphere, showing strong inter-annual variability (Jacobi et al., 1998). Investigations of the quasi 2-day wave are found for instance in studies by Salby (1981a); Rodgers and Prata (1981); Yue et al. (2012) and more recently by Tschanz and Kämpfer (2015), who analyzed the 2-day wave signatures in arctic middle-atmospheric water vapor measurements in conjunction with the occurrence of sudden stratospheric warmings. Characteristics of the 5-day wave were analyzed by Rosenlof and Thomas (1990); Wu et al. (1994); Riggin et al. (2006); Belova et al. (2008) and waves with even longer periods have been observed in the mesosphere and lower thermosphere (Forbes et al., 1995; McDonald et al., 2011; Scheiben et al., 2014; Rüfenacht et al., 2016).

Besides the presence of planetary waves, signatures of atmospheric tides (ter-diurnal, semi-diurnal, diurnal) can be seen in middle atmospheric constituents or parameters like wind, ozone, water vapor or temperature. Diurnal tides can be triggered by latent heat release within the troposphere (Hagan and Forbes, 2002) and can be of migrating or non-migrating nature. Overall complex interactions of atmospheric waves and coupling processes between different atmospheric layers exist. As Forbes (2009) assessed, the semi-diurnal solar thermal tide is a feature in the atmosphere of the earth, and serves to globally couple the troposphere, stratosphere, mesosphere, thermosphere and ionosphere.

Apart from direct observations of middle atmospheric wind as a proxy for dynamical patterns, it is common to use observations of $\mathrm{H_2O}$ that can serve as diagnostic and dynamical tracers, even from ground-based profile measurements (Liu et al., 2013; Lainer et al., 2015), due to their relative long chemical lifetime, which is on the order of weeks in the mesosphere (Brasseur and Solomon, 2006).

Here we report on ground-based observed water vapor oscillations in the mesosphere above Switzerland ($46.88\,°\mathrm{N}$, $7.46\,°\mathrm{W}$) with a period of around 18 hours and investigate the monthly mean and temporal characteristics of the wave amplitudes. This is to our knowledge the first study that explores a quasi 18-hour dominant wave mode in wintry (Northern Hemisphere) upper mesospheric conditions with passive microwave radiometric techniques. For this investigation not only ground-based water vapor data is analyzed. A mesospheric zonal wind data set from a measurement campaign at the Observatoire de Haut-Provence (OHP, $43.56\,°\mathrm{N}$, $5.43\,°\mathrm{E}$) in France with the microwave Doppler wind radiometer WIRA (Rüfenacht et al., 2014) is also considered. The focus of this paper is on the observation of atmospheric wave signatures and their temporal evolution.

In Sect. 2 the data sets from the ground-based remote sensing instruments are described. The data processing methodology and the underlying numerical approach is part of Sect. 3. Section 4 describes and analyzes the results and some distinguished features of the present 18-hour spectral component. Possible implications of the observed wave activity in our $\mathrm{H_2O}$ and wind data like an impact of inertia-gravity waves or a coupling of a quasi 2-day wave to the diurnal tide is addressed in Sect. 4.3. Final conclusions are provided in Sect. 5.

2 Instruments and data sets

The advantage of ground-based microwave radiometry is to continuously measure the amount of atmospheric trace gases at altitudes between roughly 30 and $80\,\mathrm{km}$ under most environmental conditions. Observations are possible during day, night and under cloudy conditions. The technique is widely used to study the middle atmosphere (Kämpfer et al., 2012). In this section we present the middle atmospheric water vapor radiometer MIAWARA and Doppler wind radiometer WIRA.

2.1 Middle atmospheric water vapor radiometer

The middle atmospheric water vapor radiometer MIAWARA was built in 2002 at University of Bern (Deuber et al., 2004). The Front-End of the radiometer receives emissions from the pressure broadened rotational transition line of the $\mathrm{H_2O}$ molecule at the center frequency of $22.235\,\mathrm{GHz}$. For studying oscillations with periods shorter than one day, a high temporal resolution of a few hours with an evenly spaced time series is required. In our case a MIAWARA water vapor retrieval version with a temporal resolution of 3 hours is applied. The $\mathrm{H_2O}$ retrieval from the integrated raw spectra is based on the optimal estimation method (OEM) as presented in Rodgers (2000). We use the ARTS/QPACK software (Eriksson et al., 2005, 2011), where the OEM is used to perform the inversion of the atmospheric radiative transfer model ARTS. The FFT (Fast-Fourier Transform) spectrometer in the Back-End of MIAWARA has a resolution of $60\,\mathrm{kHz}$ and the retrieval uses an overall spectrum bandwidth of $50\,\mathrm{MHz}$. A monthly mean zonal mean Aura MLS climatology provides the a priori water vapor profile and additionally Aura MLS is used to set the pressure, temperature and geopotential height in the retrieval part. MIAWARA is part of NDACC (Network for the Detection of Atmospheric Composition Change) and is persistently probing middle atmospheric $\mathrm{H_2O}$ from the Atmospheric Remote Sensing observatory in Zimmerwald ($46.88\,^{\circ}\mathrm{N}$, $7.46\,^{\circ}\mathrm{E}$, $907\,\mathrm{m}$ a.s.l.) close to Bern since 2006. In the stratosphere the vertical resolution of the water vapor profiles is $11\,\mathrm{km}$ and degrades to about $14\,\mathrm{km}$ in the mesosphere (Deuber et al., 2005). A recent validation against the Aura MLS v4.2 water vapor product (Livesey et al., 2015) revealed that for most months and altitudes the relative differences between MIAWARA and Aura MLS are below $5\,\%$ (Lainer et al., 2016).

During the winter months the tropospheric humidity is lower than during summer and in consequence the microwave signal from the middle atmosphere is less attenuated by penetrating the troposphere to the ground-based receiver. Hence an integration of the signal of only 3 hours can be used to retrieve the $\mathrm{H_2O}$ profiles. In order to characterize a retrieved $\mathrm{H_2O}$ profile the averaging kernel matrix can be used (Rodgers, 2000). This key quantity describes to what extent the retrieval is smoothing the true atmospheric state and how sensitive it is to the a priori profile (measurement response). To define a reliable altitude range for our retrieved data, we use a typical range for the threshold for the measurement response between 60–$80\,\%$.

The MIAWARA $\mathrm{H_2O}$ time series between October 2014 and March 2016 is shown in Fig. 1 with a measurement response of $80\,\%$ that is represented by the white horizontal lines. Except for some outliers we consider the upper measurement limit to range within 0.02–$0.04\,\mathrm{hPa}$ during the winter time period. In the summer season the $\mathrm{H_2O}$ retrieval from an 3 hour signal integration has a significantly lower measurement response. It is not possible to get information that is sufficiently a priori independent above approximately $0.1\,\mathrm{hPa}$ in the upper mesosphere. Further we note that we miss one week of MIAWARA data due to hardware problems beginning in the end of December 2015. This data gap is shown by a white bar in the MIAWARA $\mathrm{H_2O}$ time series.

In order to provide more information on the water vapor variability in the upper mesosphere, Figs. 2 and 3 are shown. There the monthly water vapor time series of MIAWARA averaged between 0.02–$0.1\,\mathrm{hPa}$ are plotted during the two winter time periods. It is the same altitude region where the 18-hour oscillations appeared. Later in the spectral wave analysis monthly mean wave spectra of the same months will be derived.

2.2 Doppler wind radiometer

In 2012 the novel wind radiometer WIRA (Rüfenacht et al., 2014) has been developed at the Institute of Applied Physics at the University of Bern. It is the only instrument capable to steadily observe wind in the otherwise sparsely probed atmospheric layer between 35 and $70\,\mathrm{km}$ altitude. Other techniques like rocket (Schmidlin, 1986) or lidar-based measurements (Lübken et al., 2016; Baumgarten et al., 2015) can provide wind data in this region with a higher vertical and temporal resolution than WIRA but suffer from high operational costs (rockets, lidar) or cloudy conditions (lidar). Meteorological rocket soundings are thus only suitable for short campaigns but not for continuous observations. WIRA, a ground-based passive microwave heterodyne receiver, observes the Doppler shifts of the pressure-broadened emission line of ozone at $142\,\mathrm{GHz}$. The retrieval of zonal and meridional middle atmospheric wind components is based on OEM. The measurement uncertainty ranges from 10 to $20\,\mathrm{m\,s^{-1}}$ and the vertical resolution varies between 10 and $16\,\mathrm{km}$. For more detailed information about the instrument we refer to papers by Rüfenacht et al. (2012, 2014). In order to resolve the 18-hour wave the retrieval was pushed to the limits by using measurements with an integration time of 6 hours only, instead of the usual 24-hour averages. Therefore, a new retrieval version which improves the wind accuracy of the mesospheric zonal wind estimates has been used in this study. However the data quality of the meridional wind component retrieved from 6 hourly spectral line integrations is mediocre and thus not used in our study. In order to retrieve the meridional wind in the middle atmosphere a much longer integration time, like $24\,\mathrm{h}$, is needed.

The WIRA instrument was capable to observe a quasi 18-hour zonal wind oscillation for the time period between 2013-01-25 and 2013-02-10 within the pressure range 0.1–$1\,\mathrm{hPa}$. During that time the wind radiometer was deployed at the observatory in Haute-Provence ($43.56\,°$N, $5.43\,°$E) within the scope of the ARISE (Atmospheric dynamics Research InfraStructure in Europe) project. Figure 4 shows the uninterrupted zonal wind data set as measured by WIRA between 2013-01-25 and 2013-02-10. In the whole altitude domain the measurement response of the WIRA radiometer is greater than $80\,\%$.

3 Numerical method

In order to derive the wave spectrum of the MIAWARA $\mathrm{H_2O}$ data time series, we applied the following numerical methods: A digital band-pass filter (non-recursive finite impulse response) with a comprised Hamming window is applied to the data time series to extract amplitudes of hidden oscillations of periods between 6 and 30 hours. Performing windowing methods to measurement time series ensure that the data endpoints fit together and smooth out short-term fluctuations to put longer-term cycles to foreground. Therefore the spectral leakage can be reduced (Harris, 1978). In Studer et al. (2012) the numerical structure of the band-pass filter has been shown. Lately the filter has been used to investigate the impact of the 27-day solar rotation cycle on mesospheric water vapor (Lainer et al., 2016) and to analyze the quasi 16-day planetary wave during boreal winter (Scheiben et al., 2014). We follow the advice from Oppenheim et al. (1989) and run the filter with a zero phase lag forward and backward along the measurement time series. The cut-off frequencies of the bandpass attenuation are either set to $5\,\%$ or $16.6\,\%$ (depending on the analysis method) of the initialized central frequency. The central frequency prearranges the size of the Hamming window which is the triple-fold of the central period. Our filter and window setup guarantees a fast adaptability to data variations in time.

4 Results

4.1 Monthly mean H_2O wave spectra

A mean wave amplitude is obtained by averaging amplitude series over time. For example, a final H_2O wave amplitude spectrum as presented in Fig. 5 and 6 is created by computing the monthly-averaged amplitudes as a function of the period. The period range goes from 6 to 30 hours with a spectral resolution of 1 hour. Overall, 12 months of microwave radiometric water vapor measurements were processed. The mean amplitude wave spectra reveal that except for October 2014 the highest wave amplitudes are located in the 18-hour period band for the 2014/15 period. During October 2014 a different regime close to a 12 hour period is dominating. Below $1\,\mathrm{hPa}$ amplitudes in water vapor are small. Regarding the 18-hour variability the altitude domain above $0.1\,\mathrm{hPa}$ is most interesting. During the 2015/16 period clear 18-hour signals can be found in November 2015, January and February 2016 (Fig. 6). During the other 3 months (October and December 2015, March 2016) high amplitudes show up with periods near 12 and 24 hours (tidal patterns). Clear and high wave amplitudes at exactly 18 hours are found in December 2014 (Fig. 5c), January 2016 (Fig. 6d) and February 2016 (Fig. 6e). The altitude region, where the 18-hour oscillation is prominent, is mostly above $0.1\,\mathrm{hPa}$. We find monthly mean quasi 18-hour H_2O amplitudes in the range 0.2–$0.3\,\mathrm{ppm}$. Prominent wave events with sharp 18-hour periods happened in January and February 2016. Within the subsequent section we investigate how often the 18-hour wave packets have been observed in the MIAWARA water vapor time series.

4.2 Temporal evolution of quasi 18-hour wave

We present the whole temporal evolution (12 months) of the water vapor oscillations in the quasi 18-hour period band for MIAWARA. Absolute and relative wave amplitudes, which are calculated relative to the average water vapor mixing ratio at a pressure level over the investigated time period, are presented.

Both the absolute and the relative amplitudes of the 18-hour wave in the MIAWARA observations show that this wave occurs quite regularly during the investigated winter months (Figs. 7 and 8). The amplitudes of the wave become highest above the mid-mesosphere ($0.1\,\mathrm{hPa}$). Local (in time) amplitudes reach up to $0.5\,\mathrm{ppm}$ or $12\,\%$ in relative units. Scheiben et al. (2013) showed that in the altitude range from $3\,\mathrm{hPa}$ to $0.05\,\mathrm{hPa}$ the diurnal H_2O amplitudes do not exceed $0.05\,\mathrm{ppm}$. The 18-hour H_2O wave emerges in packets and a growing of the amplitudes with decreasing pressure can be identified. Both wave characteristics could be reminiscent of inertia-gravity waves. But since the 18-hour period exceeds the inertia period for the location of Bern by about $1.5\,\mathrm{h}$ some background wind speed is required that adjusts a lower intrinsic wave period to the 18-hour period observed from ground via Doppler shifting.

From the 20th of November 2012 to the 6th of May 2013 WIRA has observed middle-atmospheric wind from the Observatoire de Haute-Provence within the district of Alpes-de-Haute-Provence in southern France. A continuous phase of 6 hourly resolved observations for about 17 days makes it possible to search for 18-hour wave activity and strong zonal wind 18-hour wave components could be identified (Fig. 9). A comparison of zonal wind and water vapor wave amplitudes could be misleading since the second highly depends on the vertical gradient. Thus such a comparison is not performed and the zonal wind analysis shown here has to be seen as an independent result and short part of the paper.

The temporal distribution of the absolute zonal wind amplitudes is shown in Fig. 9a. During the observation period the quasi 18-hour waves show now preference for certain altitudes and emerge at very different pressure levels. On 2013-02-10 the highest wave amplitudes appear between $0.1–0.2\,\mathrm{hPa}$ and reach $30–35\,\mathrm{m\,s^{-1}}$, which is about $50\,\%$ (Fig. 9b) of the mean wind speed over the 17 investigated days at these pressure levels. A second bigger wave event is located at lower altitudes (below $0.5\,\mathrm{hPa}$) and takes place between 2013-01-31 and 2013-02-03. But the relative wave amplitudes do not exceed around $30\,\%$. The appearance of these wave events is occasional and they last for a few 18-hour cycles, but not for a longer period. Qualitatively, this looks like the same behavior as revealed by the water vapor analysis. A rough estimate of the pressure layer averaged ($0.1–1\,\mathrm{hPa}$) RMSEs (Root-mean-square error) of the absolute zonal wind wave amplitudes have values between 3.3 and $6.6\,\mathrm{m\,s^{-1}}$ over the investigated time period. The temporal mean RMSE of the zonal wind amplitudes is $5.4\,\mathrm{m\,s^{-1}}$. After measuring the signal power of the WIRA zonal wind time series, white Gaussian noise was added to reach a signal to noise ratio of $5\,\mathrm{dB}$. The RMSE then was calculated from two spectral filter analyses of the noisy and original data set.

In the first part of the next Sect. 4.3 we will expand on possible MIAWARA instrument and retrieval artifacts that might have an influence on our data variability in the sub-diurnal time period. In conclusion we straighten out that the observed oscillations are robust. Later we discuss the results given in Sect. 4 in context to other performed studies related to inertia gravity wave activity and non-linear wave-wave interactions in the winter mid-latitude middle atmosphere.

4.3 Discussion

A spectral analysis of local instrument related temperatures at the MIAWARA measurement site, such as outdoor temperatures, indoor temperatures, mixer temperatures, Aquiris FFT FPGA (Field Programmable Gate Array) temperatures, Hot-Load and receiver temperatures, has been performed to see whether similar prominent 18-hour oscillations are present with a possible influence on the observed wave signatures in the $\mathrm{H_2O}$ retrieval data. The individual temperature amplitudes were examined for several months. Figure 10 shows the monthly mean temperature amplitudes for the six different parameters in January, February and March 2016. As illustrated in Fig. 6 high wave activity with periods between 15 and 21 hours were seen in January and February 2016 but not in March 2016. Local peaks in the monthly mean amplitude spectra occur close to 24 and 12 hours for T_{Outdoor}, T_{Indoor}, T_{Mixer}, T_{FPGA} and T_{Hot} representing the diurnal temperature cycle. A typical value for the receiver temperature T_{Rec}, which is a parameter for the internally generated noise power of the MIAWARA receiver, is in the order of $160\,\mathrm{K}$ and the monthly average amplitude variability between the investigated periods is below $2\,\mathrm{K}$. No distinct and strong variability can be identified in the period range between 15 and 18 hours for all temperature parameters that might effect the measured $\mathrm{H_2O}$ line spectrum at $22.235\,\mathrm{GHz}$. The atmospheric temperature profile that is used in the retrieval calculation as a forward model parameter is a 3 day average profile calculated from Aura MLS observations and thus cannot generate any regular perturbations at 18-hour time intervals to our retrievals. Another parameter that is needed for the calibration of the $\mathrm{H_2O}$

radiometer is the cold sky brightness temperature which is dependent on the opacity. The atmospheric opacity at $22.235\,\mathrm{GHz}$ is obtained from a tipping curve iteration according to Han and Westwater (2000) and was also analyzed for oscillations but only semi-diurnal and diurnal variations were found which is not unusual and related to changes in tropospheric humidity. Further, we use a monthly mean zonal mean water vapor climatology based on Aura MLS v2.2 measurements between 2004 and 2010 as a priori information in the retrieval process, that are not expected to influence the observed $\mathrm{H_2O}$ oscillations. Although the a priori itself only varies monthly the measurement response as shown by the white horizontal lines in Fig. 1 varies on a much shorter time scale. This is due to the fact that the a priori contribution, which is the sensitivity of the retrieval to the a priori profile, depends on the actual smoothing error related to a single $\mathrm{H_2O}$ profile retrieval with the integrated (in our case 3 hours) microwave line spectrum. To our knowledge it is not known how and if any short term variability of the measurement response effects the amount of retrieved water vapor. To clarify the terms a priori contribution (A_c) and measurement response (M_r) the conversion equation of these two quantities is given:

$$A_c = 100\,\% - M_r \tag{1}$$

A spectral analysis of the a priori contribution in the MIAWARA data over the whole altitude range of the radiometer (0.01–$10\,\mathrm{hPa}$) was performed. In total we show here three months in the beginning of the year 2016 (Fig. 11). All three months have mean wave amplitudes below $7\,\%$ at pressure levels above $0.1\,\mathrm{hPa}$, but the peaks are clearly outside of the quasi 18-hour period band.

Many parameter tests were performed to see whether a similar 18-hour variability could contaminate the data retrieval of the MIAWARA instrument and lead to artificial effects. This can be excluded and therefore the observed oscillations in water vapor are expected to be a real atmospheric feature. Since the focus of the paper is on water vapor we will not expand the parameter tests on the wind retrieval here. Next, a short review on possible explanations for the quasi 18-hour wave will be given.

As mentioned in Li et al. (2007), the 18-hour oscillation in mesospheric water vapor could be connected to the presence of low-frequency gravity-waves (GW), also called inertia-gravity waves, of similar apparent period. In general, gravity waves are a natural feature of a stably stratified atmosphere, where the squared Brunt-Väisälä frequency $N^2 > 0$. Gravity waves can be classified into three types, with either low, medium or high intrinsic wave angular frequencies $\hat{\omega}$ (Fritts and Alexander, 2003). The role of atmospheric gravity waves is to transport and deposit momentum by wave-breaking. Besides shear instability, GW breaking events are an important source of turbulent kinetic energy production near the mesopause (Fritts et al., 2003). As the sub-spectrum of gravity waves is large, plenty of different triggering mechanisms exist, including: Orographic lifting, spontaneous emission from jet streams and fronts, convective systems or water waves on oceans. Strong emissions of atmospheric gravity waves of low frequency (periods from a few hours to about 24 hours) were detected in the exit region of jets in the upper troposphere, as presented by Plougonven and Zhang (2014) and references therein. A coherent $10.5\,\mathrm{h}$ low-frequency GW packet with vertical wavelengths between 4–$10\,\mathrm{km}$ has been studied by Nicolls et al. (2010). They suggest a geostrophic adjustment of the tropospheric jet stream a few days before the actual observation as the main triggering mechanism of the inertia-gravity wave packet.

Li et al. (2007) described an 18-hour inertia-gravity wave. They used sodium-lidar measurements to probe the atmosphere between 80 and $110\,\mathrm{km}$. In a 80 hours lasting campaign (December 2004) observations of temperature, sodium density, zonal and meridional wind were conducted. A linear least square data fitting revealed strong amplitudes in the wind fields with a characteristic increase with altitude. Wind amplitude peaks were detected between 96 and $101\,\mathrm{km}$. The 18-hour signal was also present in temperature and sodium density, but less distinct. By applying linear wave theory, for details see e.g. Chapter 2 in Nappo (2002), an estimation of the horizontal wave propagation direction ($245°$), wavelength (about $1800\,\mathrm{km}$) and phase speed ($28\,\mathrm{m\,s^{-1}}$) could be determined for the first time with experimental data from a single instrument (Li et al., 2007). The vertical wavelengths were estimated to be between 15–$18\,\mathrm{km}$ below an altitude of $97\,\mathrm{km}$. The upper measurement limit of the MIAWARA water vapor radiometer is approximately at an altitude of $75\,\mathrm{km}$ ($0.02\,\mathrm{hPa}$) and does not reach the same altitudes as the previous mentioned sodium-lidar system. Still the vertical resolution of our instruments would be high enough to capture inertia-gravity waves with vertical wavelengths of about $20\,\mathrm{km}$ or larger. An advantage of microwave radiometers is that they can measure during day and night in a continuous operating mode and are not critically influenced by the occurrence of clouds, whereas lidar instruments usually are.

Revealing the possible observation of an 18-hour inertia-gravity wave in our measurements would require more co-located atmospheric profile measurements of both zonal and meridional wind and temperature. The main point would be to check if the vertical wavelengths are large enough to be detectable for our microwave radiometric observations with a finest vertical resolution of $10\,\mathrm{km}$. Further, in case of inertia-gravity waves with a ground related frequency of around 18 hours a specific background wind speed is required that reduces the actual intrinsic wave frequency (Doppler shifting) below the period of $16.44\,\mathrm{h}$ corresponding to the inertia frequency at the latitude of Bern.

In principle it would be possible to apply the hodograph method (Sawyer, 1961) with wind data from the WIRA radiometer and derive inertia-gravity wave parameters. During the time period when the WIRA data was analyzed for this study the instrument was not able to provide meridional winds in the temporal resolution required. Thus we were not able to derive hodographs in the upper mesosphere. We note, that a substantial number of gravity wave studies (Li et al., 2007; Plougonven and Teitelbaum, 2003; Baumgarten et al., 2015) made use of the hodograph analysis.

A Doppler wind and temperature lidar measurement campaign in northern Norway by Baumgarten et al. (2015) identified a number of inertia-gravity wave cases at altitudes between 60–$70\,\mathrm{km}$ with emphasis on upward propagation and vertical wavelengths in the range 5–$10\,\mathrm{km}$. One observed gravity wave had an apparent period of approximately 11 hours. Such a gravity wave could not be observed with our microwave radiometers due to a too low vertical resolution.

Another complication in the comparison between wind and $\mathrm{H_2O}$ wave signatures comes from oscillations in $\mathrm{H_2O}$ that may be caused by the polar vortex edge moving across the observation site. Across the polar vortex edge large meridional gradients in $\mathrm{H_2O}$ tracer concentrations exist. A regular movement of the whole vortex could therefore trigger oscillations in atmospheric $\mathrm{H_2O}$ profile measurements. Indeed we find such oscillations of the polar vortex edge during winter above Bern, but the dominant period is $24\,\mathrm{h}$ in the mesosphere (0.01–$1\,\mathrm{hPa}$). We could not find any connection to an 18-hour period we are focusing on in this study.

Besides the potential observation of inertia-gravity wave activity in our presented H_2O and zonal wind data sets, there seems to be another possibility of a non-linear wave coupling between a 2-day wave and the diurnal tide. Lieberman et al. (2017) use the global NOGAPS (Navy Operational Global Atmospheric Prediction System) ALPHA (Advanced Level Physics High Altitude) model to investigate a non-linear interaction between the migrating diurnal tide and the westward propagating quasi 2-day wave. This interaction results in a westward traveling wave component (W4) of zonal wave number 4 with an apparent period of $16\,\mathrm{h}$ and an eastward propagating wave of zonal wave number 2 with a period of 2 days. Amplitudes of W4 are largest in the mid-latitude winter mesosphere and the wind magnitudes in the MLT reach typically $10\,\mathrm{m\,s^{-1}}$ in the model data. However wind amplitudes from meteor radar measurements at Bear Lake ($42\,°\mathrm{N}$, $111.3\,°\mathrm{W}$) exceeded those from the NOGAPS ALPHA model system. The maximal zonal wind amplitudes of the 18-hour wave component observed by WIRA at a comparable latitude reach about 30–$35\,\mathrm{m\,s^{-1}}$ in the mid-mesosphere. But the lower altitude of the WIRA measurements impede an acceptable comparison to results in the paper of Lieberman et al. (2017).

The fact, that the W4 wave shows inertia-gravity wave-like features and has a period within our defined quasi 18-hour period band, it is likely that we observed such a described W4 wave in our spectral data analyses. For November 2014, February and March 2015 the monthly mean amplitude peaks in the water vapor wave spectrum is closer to $16\,\mathrm{h}$ than to $18\,\mathrm{h}$, which could be a clue for a W4 wave. In contrast to satellite observations, the temporal resolution of the local profile measurements, which our instruments provide, are not outside the Nyquist limits of temporal resolution for the westward traveling 16-hour W4 wave. The information of long-term microwave radiometric observations of non-linear wave-wave couplings such as W4 could be very useful to validate numerical model results.

5 Conclusion

For the first time a dominant quasi 18-hour wave in mesospheric water vapor has been reported from ground-based measurements. A unique data set from the MIAWARA instrument with a temporal resolution of 3 hours has been examined for wave signatures with periods between 6–30 hours. Two winter time periods were used to present monthly mean wave spectra of H_2O. For a considerable number of months prominent wave signatures in the quasi 18-hour (15–21 hours) period band have been identified. The packet-like occurrence in time and growing amplitudes with decreasing pressure are a inertia-gravity wave-like feature.

In the first part of Sect. 4.3 we clarified that our ground-based observations are robust and that the retrievals are not contaminated by any considerable artifacts. Whether the observed wave is a direct image of a low frequency inertia-gravity wave is not definitely clear, but gravity waves with comparable frequencies have been observed at mesospheric altitudes in the winter hemisphere. Another promising clarification approach is the mentioned non-linear coupling of the quasi 2-day wave to the migrating diurnal tide. A much more detailed analysis of the quasi 2-day wave behavior above Bern is necessary to understand the complex interactions and wave couplings we identified in mesospheric water vapor and zonal wind profile time series. This is an encouraging future research project.

It has been shown that the Doppler wind radiometer WIRA is capable to resolve sub-diurnal oscillations in the zonal wind component. The quality of the meridional wind measurements have a potential for improvement and could contribute to wave characteristic analyses in the near future. Quasi 18-hour oscillations were detected in the WIRA zonal wind data set for a period of about 17 days. There are also meteor radar based measurements (Huang et al., 2013), where similar wave periods ($\sim 16\,\mathrm{h}$) are observed. At the very least the different wind observations could provide an additional constraint for 3-dimensional model simulation studies achievable with for instance WACCM (Whole Atmosphere Community Climate Model) or ECHAM. A useful exercise could aim at validating the correct representation of non-linear wave-wave couplings in different models involving tides and planetary waves like the quasi 2-day wave.

Author contributions. ML was responsible for the ground-based water vapor measurements, performed the data analysis and prepared the manuscript. KH designed the filter algorithm and contributed to the interpretation of the results. RR is in charge of WIRA, the ground based wind radiometer, and provided wind retrieval data. NK is the lead of the project group. All authors read and approved the current version of the manuscript and declare that they have no conflict of interest.

Acknowledgements. This work is supported by Swiss National Science Foundation Grant 200020-160048 and MeteoSwiss in the frame of the GAW project “Fundamental GAW parameters measured by microwave radiometry”. Rolf Rüfenacht is supported by Post-doc Grant P2PEB2-165383. The authors acknowledge NASA for access to Aura MLS data and are grateful for constructive comments provided during the review process.

References

Baumgarten, G., Fiedler, J., Hildebrand, J., and Lübken, F.-J.: Inertia gravity wave in the stratosphere and mesosphere observed by Doppler wind and temperature lidar, Geophys. Res. Lett., 42, 10,929–10,936, doi:10.1002/2015GL066991, 2015GL066991, 2015.

Belova, A., Kirkwood, S., Murtagh, D., Mitchell, N., Singer, W., and Hocking, W.: Five-day planetary waves in the middle atmosphere from Odin satellite data and ground-based instruments in Northern Hemisphere summer 2003, 2004, 2005 and 2007, Ann. Geophys., 26, 3557–3570, doi:10.5194/angeo-26-3557-2008, 2008.

Brasseur, G. and Solomon, S.: Aeronomy of the Middle Atmosphere: Chemistry and Physics of the Stratosphere and Mesosphere, vol. 32, Springer, 2006.

Deuber, B., Kämpfer, N., and Feist, D. G.: A new 22-GHz Radiometer for Middle Atmospheric Water Vapour Profile Measurements, IEEE Trans. Geosci. Remote Sens., 42, 974–984, doi:10.1109/TGRS.2004.825581, 2004.

Deuber, B., Haefele, A., Feist, D. G., Martin, L., Kämpfer, N., Nedoluha, G. E., Yushkov, V., Khaykin, S., Kivi, R., and Vomel, H.: Middle Atmospheric Water Vapour Radiometer - MIAWARA: Validation and first results of the LAUTLOS / WAVVAP campaign, J. Geophys. Res., 110, D13 306, doi:10.1029/2004JD005543, 2005.

Eriksson, P., Jiménez, C., and Buehler, S. A.: Qpack, a general tool for instrument simulation and retrieval work, J. Quant. Spectrosc. Radiat. Transfer, 91, 47 – 64, doi:10.1016/j.jqsrt.2004.05.050, 2005.

Eriksson, P., Buehler, S., Davis, C., Emde, C., and Lemke, O.: ARTS, the atmospheric radiative transfer simulator, version 2, J. Quant. Spectrosc. Radiat. Transfer, 112, 1551 – 1558, doi:10.1016/j.jqsrt.2011.03.001, 2011.

Forbes, J. M.: Vertical coupling by the semidiurnal tide in Earth's atmosphere, Annual reviews, 2009.

Forbes, J. M., Hagan, M. E., Miyahara, S., Vial, F., Manson, A. H., Meek, C. E., and Portnyagin, Y. I.: Quasi 16-day oscillation in the mesosphere and lower thermosphere, J. Geophys. Res. Atmos., 100, 9149–9163, doi:10.1029/94JD02157, 1995.

Fritts, D. C. and Alexander, M. J.: Gravity wave dynamics and effects in the middle atmosphere, Rev. Geophys., 41, doi:10.1029/2001RG000106, 1003, 2003.

Fritts, D. C., Bizon, C., Werne, J. A., and Meyer, C. K.: Layering accompanying turbulence generation due to shear instability and gravity-wave breaking, J. Geophys. Res. Atmos., 108, doi:10.1029/2002JD002406, 8452, 2003.

Hagan, M. E. and Forbes, J. M.: Migrating and nonmigrating diurnal tides in the middle and upper atmosphere excited by tropospheric latent heat release, J. Geophys. Res. Atmos., 107, ACL 6–1–ACL 6–15, doi:10.1029/2001JD001236, 4754, 2002.

Han, Y. and Westwater, E. R.: Analysis and improvement of tipping calibration for ground-based microwave radiometers, IEEE Transactions on Geoscience and Remote Sensing, 38, 1260–1276, doi:10.1109/36.843018, 2000.

Hardiman, S. C., Butchart, N., Charlton-Perez, A. J., Shaw, T. A., Akiyoshi, H., Baumgaertner, A., Bekki, S., Braesicke, P., Chipperfield, M., Dameris, M., Garcia, R. R., Michou, M., Pawson, S., Rozanov, E., and Shibata, K.: Improved predictability of the troposphere using stratospheric final warmings, J. Geophys. Res. Atmos., 116, doi:10.1029/2011JD015914, d18113, 2011.

Harris, F. J.: On the use of windows for harmonic analysis with the discrete Fourier transform, Proc. IEEE, 66, 51–83, doi:10.1109/PROC.1978.10837, 1978.

Huang, K. M., Liu, A. Z., Lu, X., Li, Z., Gan, Q., Gong, Y., Huang, C. M., Yi, F., and Zhang, S. D.: Nonlinear coupling between quasi 2 day wave and tides based on meteo radar observations at Mauri, Journal of Geophysical Research: Atmospheres, 118, 10,936–10,943, doi:10.1002/jgrd.50872, 2013JD020086, 2013.

Jacobi, C., Schminder, R., and Kürschner, D.: Planetary wave activity obtained from long-period (2–18 days) variations of mesopause region winds over Central Europe (52 °N, 15 °E), J. Atmos. Sol.-Terr. Phy., 60, 81–93, doi:10.1016/S1364-6826(97)00117-X, 1998.

Kämpfer, N., Nedoluha, G., Haefele, A., and De Wachter, E.: Microwave Radiometry, vol. 10 of *ISSI Scientific Report Series*, Springer New York, doi:10.1007/978-1-4614-3909-7, 2012.

Lainer, M., Kämpfer, N., Tschanz, B., Nedoluha, G. E., Ka, S., and Oh, J. J.: Trajectory mapping of middle atmospheric water vapor by a mini network of NDACC instruments, Atmos. Chem. Phys., 15, 9711–9730, doi:10.5194/acp-15-9711-2015, 2015.

Lainer, M., Hocke, K., and Kämpfer, N.: Variability of mesospheric water vapor above Bern in relation to the 27-day solar rotation cycle, J. Atmos. Sol.-Terr. Phy., 143–144, 71–87, doi:http://dx.doi.org/10.1016/j.jastp.2016.03.008, 2016.

Li, T., She, C.-Y., Liu, H.-L., Leblanc, T., and McDermid, I. S.: Sodium lidar–observed strong inertia-gravity wave activities in the mesopause region over Fort Collins, Colorado (41°N, 105°W), J. Geophys. Res. Atmos., 112, doi:10.1029/2007JD008681, d22104, 2007.

Lieberman, R. S., Riggin, D. M., Nguyen, V., Palo, S. E., Siskind, D. E., Mitchell, N. J., Stober, G., Wilhelm, S., and Livesey, N. J.: Global observations of 2 day wave coupling to the diurnal tide in a high-altitude forecast-assimilation system, Journal of Geophysical Research: Atmospheres, 122, 4135–4149, doi:10.1002/2016JD025144, 2016JD025144, 2017.

Liu, J., Tarasick, D. W., Fioletov, V. E., McLinden, C., Zhao, T., Gong, S., Sioris, C., Jin, J. J., Liu, G., and Moeini, O.: A global ozone climatology from ozone soundings via trajectory mapping: a stratospheric perspective, Atmos. Chem. Phys., 13, 11 441–11 464, doi:10.5194/acp-13-11441-2013, 2013.

Livesey, N. J., Read, W. G., Wagner, P. A., Froidevaux, L., Lambert, A., Manney, G. L., Millán Valle, L. F., Pumphrey, H. C., Santee, M. L., Schwartz, M. J., Wang, S., Fuller, R. A., Jarnot, R. F., Knosp, B. W., and Martinez, E.: Version 4.2x Level 2 data quality and description document, Tech. rep., Jet Propulsion Laboratory, California Institute of Technology, 2015.

Lübken, F.-J., Baumgarten, G., Hildebrand, J., and Schmidlin, F. J.: Simultaneous and co-located wind measurements in the middle atmosphere by lidar and rocket-borne techniques, Atmospheric Measurement Techniques, 9, 3911–3919, doi:10.5194/amt-9-3911-2016, 2016.

McDonald, A. J., Hibbins, R. E., and Jarvis, M. J.: Properties of the quasi 16 day wave derived from EOS MLS observations, J. Geophys. Res. Atmos., 116, D06 112, doi:10.1029/2010JD014719, 2011.

Nappo, C. J.: An introduction to atmospheric gravity waves, Academic Press, 2002.

Nicolls, M. J., Varney, R. H., Vadas, S. L., Stamus, P. A., Heinselman, C. J., Cosgrove, R. B., and Kelley, M. C.: Influence of an inertia-gravity wave on mesospheric dynamics: A case study with the Poker Flat Incoherent Scatter Radar, J. Geophys. Res. Atmos., 115, doi:10.1029/2010JD014042, 2010.

Oppenheim, A. V., Schafer, R. W., Buck, J. R., et al.: Discrete-time signal processing, vol. 2, Prentice-hall Englewood Cliffs, 1989.

Orr, A., Bechtold, P., Scinocca, J., Ern, M., and Janiskova, M.: Improved Middle Atmosphere Climate and Forecasts in the ECMWF Model through a Nonorographic Gravity Wave Drag Parameterization, J. Climate, 23, 5905–5926, doi:10.1175/2010JCLI3490.1, 2010.

Plougonven, R. and Teitelbaum, H.: Comparison of a large-scale inertia-gravity wave as seen in the ECMWF analyses and from radiosondes, Geophys. Res. Lett., 30, doi:10.1029/2003GL017716, 1954, 2003.

Plougonven, R. and Zhang, F.: Internal gravity waves from atmospheric jets and fronts, Rev. Geophys., 52, 33–76, doi:10.1002/2012RG000419, 2014.

Riggin, D. M., Liu, H.-L., Lieberman, R. S., Roble, R. G., III, J. M. R., Mertens, C. J., Mlynczak, M. G., Pancheva, D., Franke, S. J., Murayama, Y., Manson, A. H., Meek, C. E., and Vincent, R. A.: Observations of the 5-day wave in the mesosphere and lower thermosphere, J. Atmos. Sol.-Terr. Phy., 68, 323 – 339, doi:10.1016/j.jastp.2005.05.010, 2006.

Rodgers, C. D.: Inverse methods for atmospheric sounding: theory and practice, vol. 2, World Scientific Publishing Co Pte. Ltd., 2000.

Rodgers, C. D. and Prata, A. J.: Evidence for a traveling two-day wave in the middle atmosphere, J. Geophys. Res. Oceans, 86, 9661–9664, doi:10.1029/JC086iC10p09661, 1981.

Rosenlof, K. H. and Thomas, R. J.: Five-day mesospheric waves observed in Solar Mesosphere Explorer ozone, J. Geophys. Res. Atmos., 95, 895–899, doi:10.1029/JD095iD01p00895, 1990.

Rüfenacht, R., Kämpfer, N., and Murk, A.: First middle-atmospheric zonal wind profile measurements with a new ground-based microwave Doppler-spectro-radiometer, Atmos. Meas. Tech., 5, 2647–2659, doi:10.5194/amt-5-2647-2012, 2012.

Rüfenacht, R., Murk, A., Kämpfer, N., Eriksson, P., and Buehler, S. A.: Middle-atmospheric zonal and meridional wind profiles from polar, tropical and midlatitudes with the ground-based microwave Doppler wind radiometer WIRA, Atmos. Meas. Tech., 7, 4491–4505, doi:10.5194/amt-7-4491-2014, 2014.

Rüfenacht, R., Hocke, K., and Kämpfer, N.: First continuous ground-based observations of long period oscillations in the vertically resolved wind field of the stratosphere and mesosphere, Atmospheric Chemistry and Physics, 16, 4915–4925, doi:10.5194/acp-16-4915-2016, 2016.

Salby, M. L.: The 2-day wave in the middle atmosphere: Observations and theory, J. Geophys. Res. Oceans, 86, 9654–9660, doi:10.1029/JC086iC10p09654, 1981a.

Salby, M. L.: Rossby Normal Modes in Nonuniform Background Configurations. Part I: Simple Fields, J. Atmos. Sci., 38, 1803–1826, doi:10.1175/1520-0469(1981)038<1803:RNMINB>2.0.CO;2, 1981b.

Sawyer, J. S.: Quasi-periodic wind variations with height in the lower stratosphere, Quart. J. Roy. Meteor. Soc., 87, 24–33, doi:10.1002/qj.49708737104, 1961.

Scheiben, D., Schanz, A., Tschanz, B., and Kämpfer, N.: Diurnal variations in middle-atmospheric water vapor by ground-based microwave radiometry, Atmospheric Chemistry and Physics, 13, 6877–6886, doi:10.5194/acp-13-6877-2013, 2013.

Scheiben, D., Tschanz, B., Hocke, K., Kämpfer, N., Ka, S., and Oh, J. J.: The quasi 16-day wave in mesospheric water vapor during boreal winter 2011/2012, Atmos. Chem. Phys., 14, 6511–6522, doi:10.5194/acp-14-6511-2014, 2014.

Schmidlin, F. J.: Rocket techniques used to measure the neutral atmosphere, Middle Atmosphere Program, Handbook for MAP, 19, R. A. Goldberg, 1–33, SCOSTEP Secretariat, Univ. of Ill., Urbana, 1986.

Studer, S., Hocke, K., and Kämpfer, N.: Intraseasonal oscillations of stratospheric ozone above Switzerland, J. Atmos. Sol.-Terr. Phy., 74, 189 – 198, doi:10.1016/j.jastp.2011.10.020, 2012.

Tschanz, B. and Kämpfer, N.: Signatures of the 2-day wave and sudden stratospheric warmings in Arctic water vapour observed by ground-based microwave radiometry, Atmos. Chem. Phys., 15, 5099–5108, doi:10.5194/acp-15-5099-2015, 2015.

Wu, D. L., Hays, P. B., and Skinner, W. R.: Observations of the 5-day wave in the mesosphere and lower thermosphere, Geophys. Res. Lett., 21, 2733–2736, doi:10.1029/94GL02660, 1994.

Yue, J., Liu, H.-L., and Chang, L. C.: Numerical investigation of the quasi 2 day wave in the mesosphere and lower thermosphere, J. Geophys. Res. Atmos., 117, D05 111, doi:10.1029/2011JD016574, 2012.

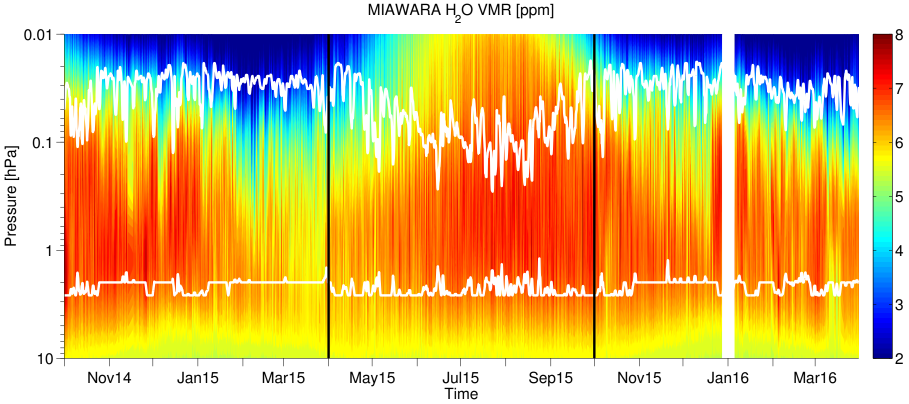

Figure 1. The water vapor volume mixing ratio [ppm] time series measured by MIAWARA between October 2014 and March 2016. The horizontal white lines indicate at which pressure levels the measurement response drops below $80\,\%$. During the more humid and warm season between April and September 2015 the data will not be used. This is marked by the vertical black lines. A measurement gap occurred between 2015-12-28 and 2016-01-04 as shown by the white bar.

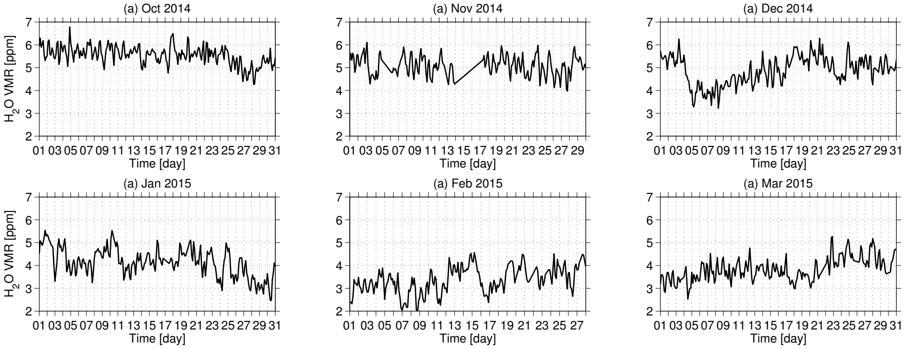

Figure 2. Monthly time series of MIAWARA $\mathrm{H_2O}$ [ppm] averaged between 0.02 and $0.1\,\mathrm{hPa}$ for winter 2014/2015.

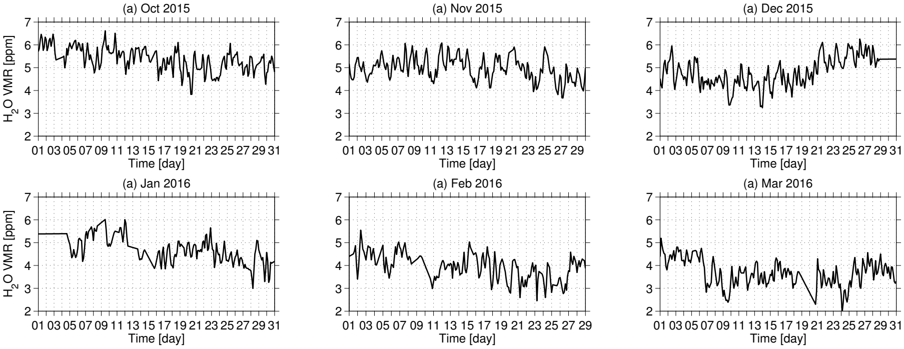

Figure 3. Same as Fig. 2, but for winter 2015/2016.

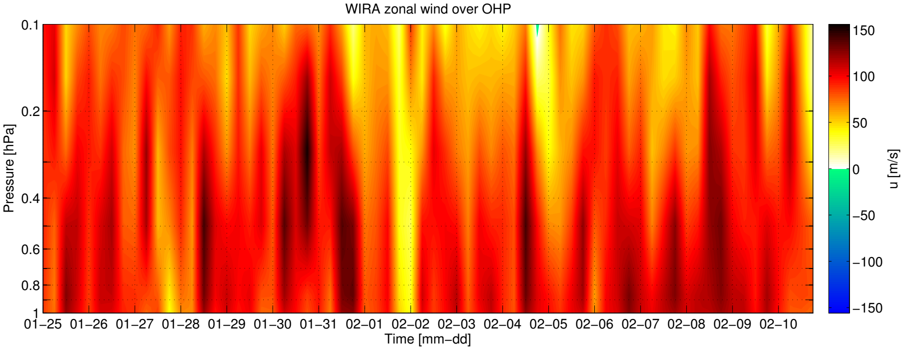

Figure 4. The zonal wind vector component time series $[\mathrm{m\,s^{-1}}]$ measured by WIRA between 2013-01-25 and 2013-02-10 in the pressure range 0.1–$1\,\mathrm{hPa}$ at the Observatoire de Haute-Provence (OHP) in France.

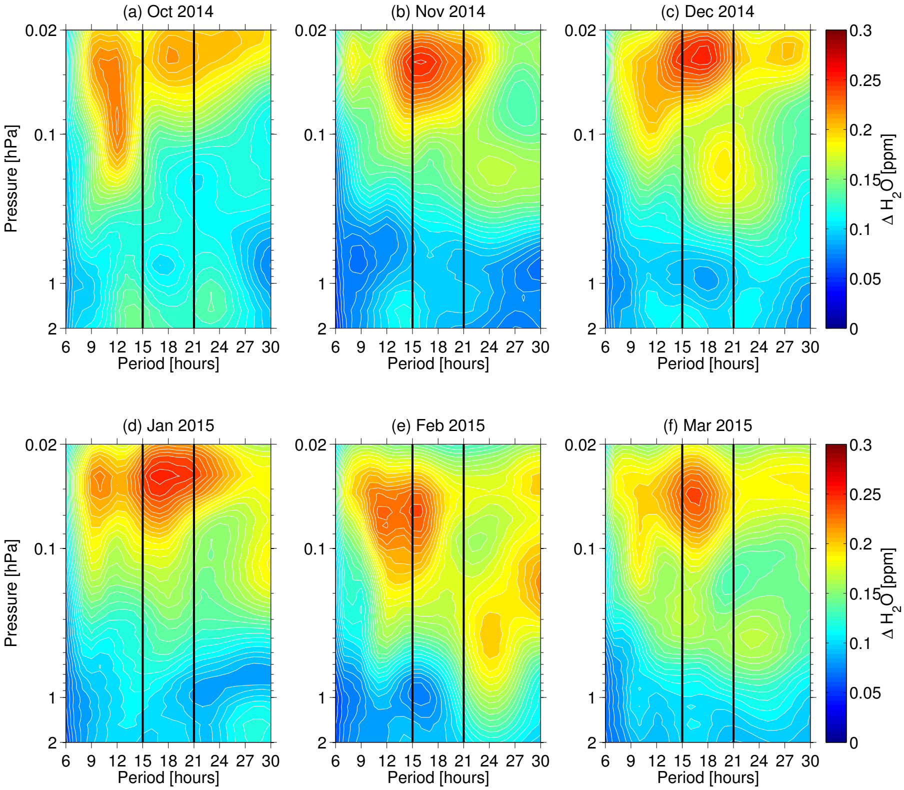

Figure 5. The MIAWARA water vapor monthly mean wave spectrum with periods between 6 and 30 hours. Shown is the result of the $\mathrm{H_2O}$ amplitudes [ppm] for the months October 2014 to March 2015 (a–f). The border of the quasi 18-hour period band (15–21 hours) is indicated by the vertical black line pair.

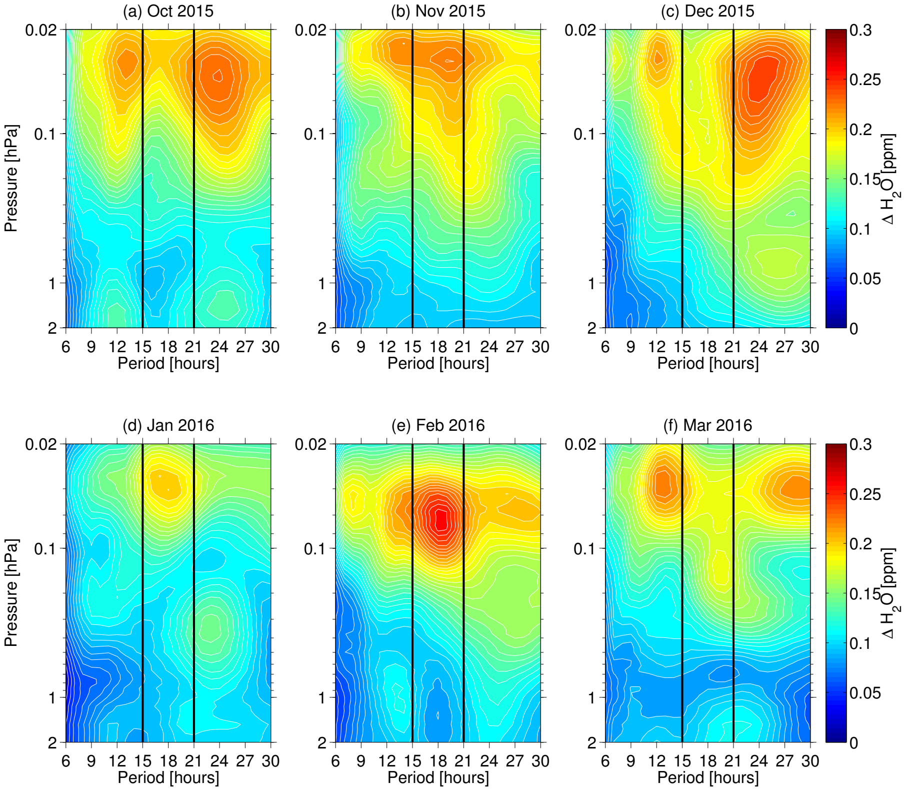

Figure 6. Same as Fig. 5, but for the months October 2015 to March 2016 (a–f).

(a) MIAWARA H_2O (15–21hr BF) amplitude

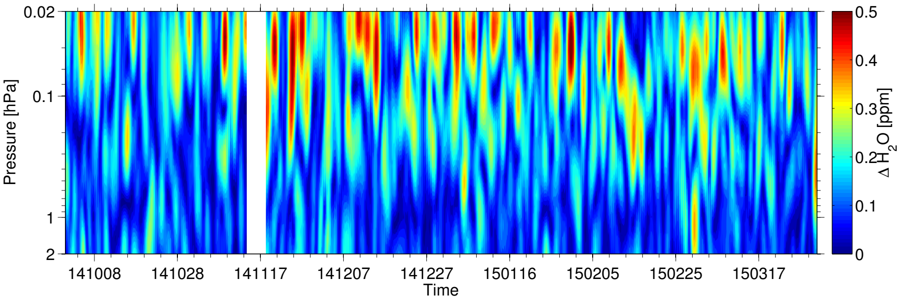

(b) MIAWARA H_2O (15–21hr BF) relative amplitude

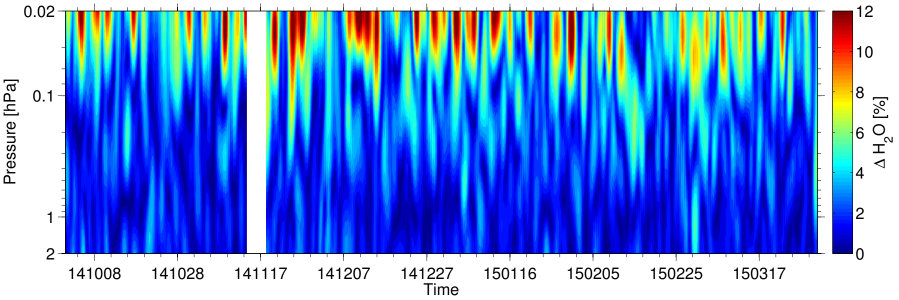

Figure 7. Temporal evolution of wave amplitudes derived from band-pass hamming-window filtered MIAWARA H_2O VMR time series with cut-off periods at 15 and 21 hours. Shown is the time period from October 2014 to March 2015.

(a) MIAWARA H_2O (15–21hr BF) amplitude

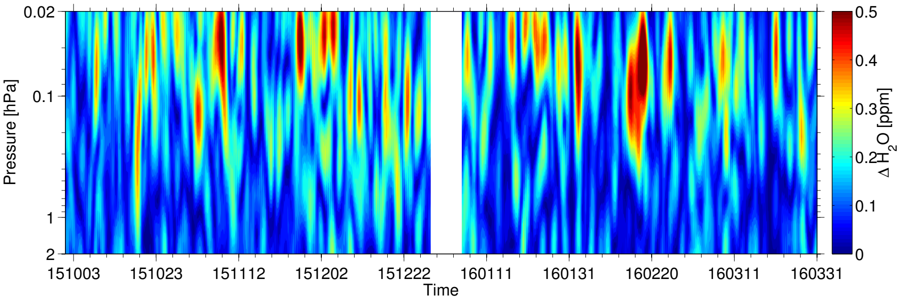

(b) MIAWARA H_2O (15–21hr BF) relative amplitude

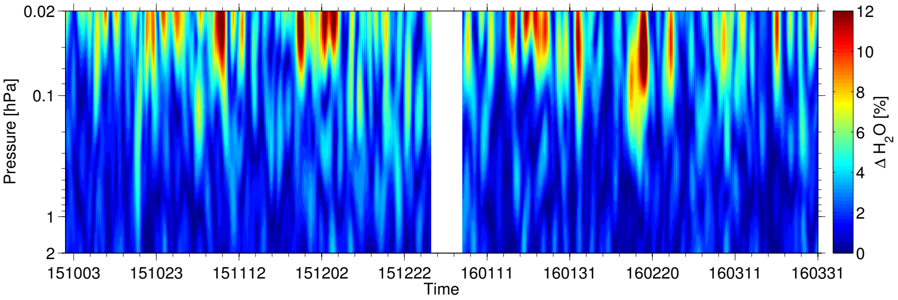

Figure 8. Same as Fig. 7, but here the time period from October 2015 to March 2016 is shown. The measurement gap between 2015-12-28 and 2016-01-04 is indicated by the white bar.

(a) WIRA zonal wind (15–21hr BF) amplitude

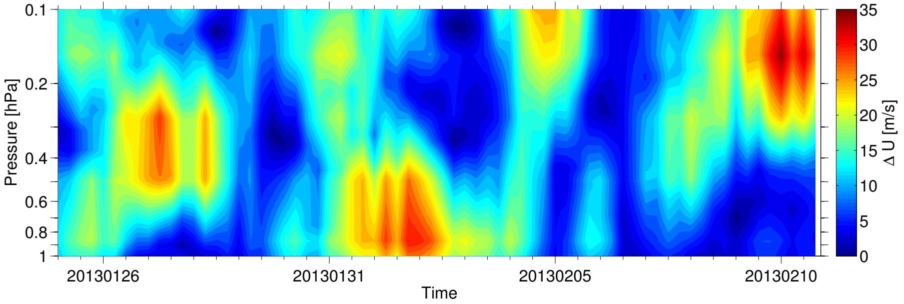

(b) WIRA zonal wind (15–21hr BF) relative amplitude

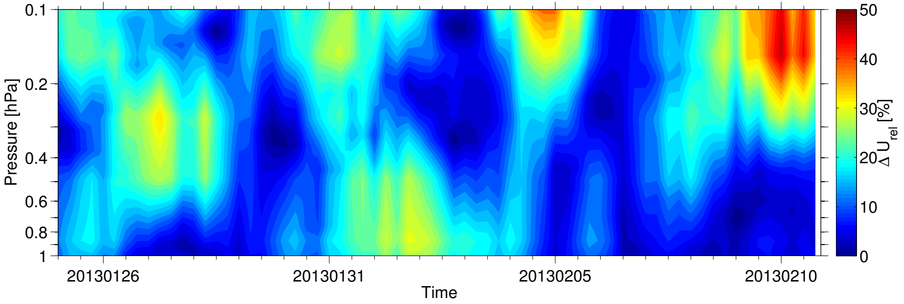

Figure 9. WIRA zonal wind band-pass filtered (15–21 h) absolute (a) and relative (b) wave amplitudes in the pressure range 0.1–1 hPa between 2013-01-25 and 2013-02-10.

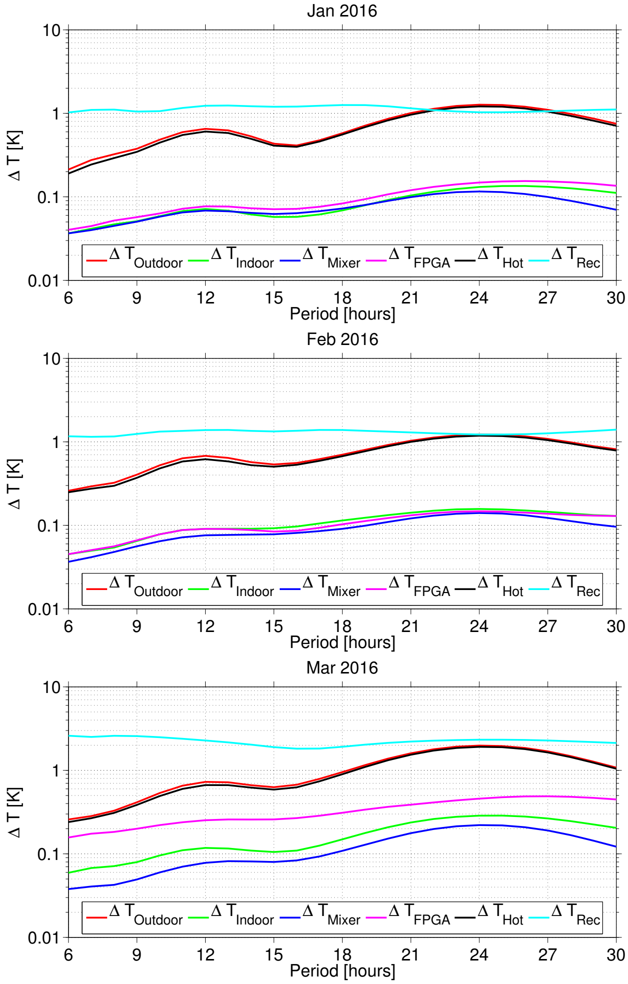

Figure 10. Monthly mean spectral wave analysis for 6 different temperature parameters related to the MIAWARA water vapor radiometer: outdoor, indoor, mixer, FPGA, Hot-Load and receiver temperature. Spectral analysis goes from 6 to 30 hours with a resolution of 1 hour. The results are shown for January, February and March 2016.

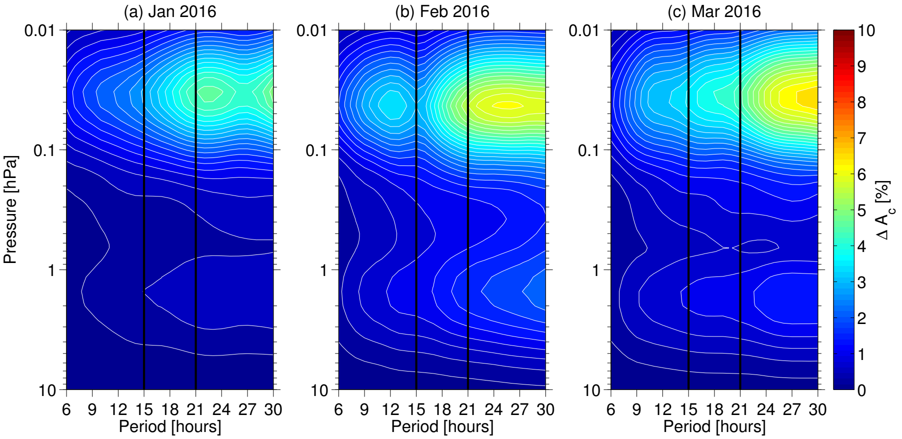

Figure 11. Spectral analysis of the a priori contribution in the MIAWARA water vapor retrievals for periods between 6 and 30 hours. Shown are monthly mean absolute wave amplitudes of the a priori contribution A_c in [%] for January (a), February (b) and March (c) 2016.